Molecular dynamics simulation of the fragile glass former orthoterphenyl: A flexible molecule model. II. Collective dynamics

S. Mossa,[1,2] G. Ruocco,[2] and M. Sampoli[3]
[1]*Center for Polymer Studies and Department of Physics, Boston University, Boston, Massachusetts 02215*
[2]*Dipartimento di Fisica and Istituto Nazionale di Fisica per la Materia, Università di Roma La Sapienza, Piazzale Aldo Moro 2, Roma, I-00185, Italy*
[3]*Dipartimento di Energetica and INFM, Università di Firenze, Via Santa Marta 3 , Firenze I-50139, Italy*
(Received 27 December 2000; revised manuscript received 27 March 2001; published 24 July 2001)

We present a molecular dynamics study of the collective dynamics of a model for the fragile glass former orthoterphenyl. In this model, introduced by Mossa, Di Leonardo, Ruocco, and Sampoli [Phys. Rev. E **62**, 612 (2000)], the intramolecular interaction among the three rigid phenyl rings is described by a set of force constants whose value has been fixed in order to obtain a realistic isolated molecule spectrum. The interaction between different molecules is described by a Lennard Jones site-site potential. We study the behavior of the coherent scattering functions $F_t(q,t)$, considering the density fluctuations of both molecular and phenyl-ring centers of mass; moreover we directly simulate the neutron scattering spectra taking into account both the contributions due to carbon and hydrogens atoms. We compare our results with the main predictions of the mode-coupling theory and with the available coherent neutron scattering experimental data.

DOI: 10.1103/PhysRevE.64.021511 PACS number(s): 64.70.Pf, 71.15.Pd, 61.25.Em, 61.20.−p

I. INTRODUCTION

The understanding of the supercooled liquid and glassy phases in molecular systems is, nowadays, one of the main tasks of the physics of disordered materials (see [1,2] and references therein for a general review). Two main theories provide us a description of the glass transition, respectively, from a thermodynamical and dynamical point of view.

The first one (see [3] and references therein) is based on first-principles computation of the *equilibrium* thermodynamics of glasses and considers the glass transition as a true thermodynamic transition. In this context, the onset of the glassy state is associated with an entropy crisis, i.e., the vanishing of the *configurational* entropy of the thermodynamically relevant states.

The second approach is the mode-coupling theory (MCT) [4,5], which studies the long-time structural dynamics and its relation with the glass transition; in this context this transition has to be considered not as a regular thermodynamical phase transition involving singularities of some observables, but as a kinetically induced transition from an ergodic to a nonergodic behavior. The structural dynamics becomes so ''slow'' that the system of interest appeared frozen on the experimental time scales.

On the experimental side, the collective dynamics of a huge variety of molecular systems has been investigated by means of several experimental techniques; colloids [6,7] and ortho-terphenyl (OTP) [8–11] are the most widely studied *fragile* [1] supercooled liquids. They are only examples of an enormous experimental work (the interested reader is referred to Ref. [2] for an accurate comprehensive review). Moreover, in the last ten years the analysis of experimental results has been flanked by extensive use of numerical techniques, mainly molecular dynamics (MD) and Monte Carlo simulations. The almost exponential growth of computational capabilities allows us to reach simulation times of the order of microseconds for simple monoatomics systems and of several tens of nanoseconds in the case of complex molecular systems; such performances definitely permit comparisons of numerical results with the structural very-long-time properties of the real systems. We remember, among many others, the results concerning the structural dynamics of two molecular liquids like simple point charge extended (SPC/E) water [12] and OTP [13,14]. We emphasize here the fact that the models involved in these studies are *molecular* and *rigid* in the sense that they have a structure and take into account the orientational properties of the molecules, but they disregard the role played by internal degrees of freedom on the overall dynamical behavior of the system.

In a recent paper [15] we have introduced a new model for the intramolecular dynamics of orthoterphenyl ($T_m = 329$ K, $T_c \simeq 290$ K, $T_g = 243$ K), one of the most deeply studied substances in the liquid, supercooled, and glassy state. The introduction of such a flexible model allows us to understand the role of internal degrees of freedom in the short-time (*fast*) dynamics [16] taking place on the time scale of a few picoseconds and to study their possible coupling with the long-time center of mass dynamics [17]. Moreover, it would allow us to emphasize once more the universality of the MCT approach for supercooled liquids and, in particular, of its molecular version in the case of complex molecular liquids. In Ref. [15] we introduced in detail the intermolecular model and we showed some results based on MD calculations; the self- (one-particle) dynamical properties of a system composed of 108 molecules have been studied in details and we have found good agreement with the main predictions of the MCT and with the experimental results related to the self-intermediate-scattering function [18,19] and the self-diffusion [20,21]. In the present paper we complete the picture considering the collective highly cooperative structural dynamics controlling the rearrangement of big portions of the system. We describe the dynamics of the molecules at the level of the molecular center of mass and at the level of the

phenyl-ring center of mass. Moreover, we calculate the neutron coherent scattering function taking into account both the contributions due to carbon and hydrogen atoms in order to make a direct comparison with the experimental results.

The paper is organized as follows. In Sec. II we summarize the main predictions of the MCT and we give a schematic introduction to the molecular mode-coupling theory (MMCT). In Sec. III we briefly describe the model and we recall some computational details. In Sec. IV we study the temperature and momentum dependence of the collective dynamics of the molecular and of the phenyl-ring centers of mass. In Sec. V we make a deep comparison between the experimental results of neutron scattering and the simulated neutron spectra calculated taking into account the interactions with both carbon and hydrogen atoms. Finally, Sec. VI contains a discussion of the results obtained and some conclusions.

II. MODE-COUPLING AND MOLECULAR MODE-COUPLING THEORY

As we have already stressed in Sec. I, two main theories, one intrinsically thermodynamical [3] and the other purely dynamical [4,5], have been developed up to now to describe the phenomenology observed in the glass transition. In this paper we will make a comparison of our numerical results with the main predictions of MCT about the center of mass structural relaxation dynamics. The reason for this is twofold: first of all this is, indeed, the theory taking into account the states actually accessible by the system on the time scale of a typical simulation. Moreover, even if some experimental results, like the presence of the so-called knee characterizing the low-frequency behavior of the light scattering susceptibility [22,23] or the presence of a cusp in the nonergodicity parameter [24], seem to contradict some of its predictions, such a theory has been verified to hold for different experimental data on a very wide time region. Finally, in the last two years successful efforts have been made in order to generalize the theory to liquids of *rigid* molecules of *arbitrary shape* [25] (see also Ref. [26] for the particular case of a liquid of *linear* rigid molecules) taking into account both translational and rotational dynamics.

In Ref. [15] we have summarized the main predictions of the so-called *ideal* MCT so that here we recall only the fundamental equations of the theory, concerning the *collective intermediate scattering function* that we will use in the following sections. MCT interprets the glass formation as a *dynamical transition* from an ergodic to nonergodic behavior at a crossover temperature T_c; the theory is written as a self-consistent dynamical treatment [4] of the intermediate scattering function, i.e., the time correlation of the density fluctuations of momentum q.

This theoretical scheme can be considered as the mathematical description of the physical picture of the *cage effect*. Following the dynamics of a tagged particle it is possible to recognize two main dynamical regions. On a small time scale of the order of some picoseconds (the β region), the dynamics of the particle is confined into a limited region (the cage) built up by the nearest neighbors. In this regime it is possible to write the intermediate scattering function as

$$F(q,t)=f(q)+h(q)\sqrt{\frac{|T-T_c|}{T_c}}G_{\pm}(t/\tau_\sigma) \tag{1}$$

where $f(q)$ is the *nonergodicity parameter* (also referred to as the *Debye-Waller factor*), $h(q)$ is an amplitude independent of temperature and time and the $\pm$ in $G_{\pm}$ corresponds to time larger or smaller with respect to τ_σ, a parameter that fixes the time scale of the β process. At this stage, the time dependence of the correlation functions is all embedded in the *q-independent* function $G_{\pm}$. $G_{\pm}(t)$ is asymptotically expressed by two power laws, respectively, the *critical decay*

$$G_+(t/\tau_\sigma)=(t/\tau_\sigma)^{-a}, \quad \tau_0 \ll t \ll \tau_\sigma \tag{2}$$

and the *von Schweidler law*,

$$G_-(t/\tau_\sigma)=-(t/\tau_\sigma)^{b}, \quad \tau_\sigma \ll t \ll \tau_\alpha; \tag{3}$$

characterized by the *temperature- and momentum-independent* exponents a and b; here τ_α is the *structural relaxation time*.

At time scales of order of τ_α the cages start to break down and the particle starts to diffuse approaching pure brownian motion. This long-time part of the dynamics is the so-called α region and is well described by a stretched exponential function

$$F(q,t)\simeq f(q)\exp\left\{-\left(\frac{t}{\tau_\alpha}\right)^{\beta_\alpha}\right\}, \tag{4}$$

which verifies the *time-temperature superposition principle* (TTSP). The α time scale τ_α depends on temperature trough a power law of the form

$$\tau_\alpha \propto (T-T_c)^{-\gamma}. \tag{5}$$

The momentum dependence of the dynamical parameters in the collective dynamics case is not trivial as in the single-particle case. When looking at the structural collective dynamics, studying different values of the momentum q means studying the highly cooperative time evolution of cages of average dimension $2\pi/q$; it is clear that such time evolution is strongly coupled to the static topological structure of the system. More precisely, MCT predicts that the parameters $f(q)$, $h^{-1}(q)$, β_α, and $\tau_\alpha(q)$ oscillate *in phase* with the static structure factor $S(q)$.

The result concerning the momentum dependence of the collective relaxation time is quite general and is well known as *de Gennes narrowing* [27]. A general relation [28] holds among the one-particle τ_s and the collective τ_c relaxation times, namely, $\tau_c(q)\simeq S(q)\tau_s(q)$; if the diffusion limit is appropriate for $F_s(q,t)$, i.e., for values of q close to the first peak of the static structure factor, we obtain

$$\tau_c(q,T)\simeq \frac{1}{D(T)}\frac{S(q)}{q^2} \tag{6}$$

where $D(T)$ is the diffusion coefficient at temperature T and $S(q)$ is supposed to be nearly temperature independent.

In summary, the momentum dependence of the collective dynamics is nontrivially driven by the static structure of the system. In particular, for *molecular* systems, the small length scale structure is determined by orientational properties of the single molecules; a pure molecular translational dynamics will, obviously, loose all the dynamical features controlled by the high momentum part of the static structure factor.

An important step toward a correct explanation of the dynamics of molecular systems is to write down a MMCT [25,26] taking into account both translational and rotational degrees of freedom. If we consider a system of N identical *rigid* molecules of arbitrary shape described by their center of mass positions $\bar{r}_j(t)$ and by the Euler angles $\Omega_j(t) = (\phi_j(t), \theta_j(t), \chi_j(t))$ we can write the time-dependent microscopic one-particle density as

$$\rho(\bar{r},\Omega,t) = \sum_{n=1}^{N} \delta[\bar{r} - \bar{r}_n(t)]\,\delta[\Omega,\Omega_n(t)]. \tag{7}$$

Expanding with respect to the complete set of functions given by the plane waves and the Wigner matrices $D^l_{mn}(\Omega)$, we have the *tensorial* density modes

$$\rho_{lmn}(\bar{q},t) = i^l (2l+1)^{1/2} \sum_{n=1}^{N} e^{i\bar{q}\cdot\bar{r}_n(t)} D^{l*}_{mn}[\Omega_n(t)]. \tag{8}$$

Then, the generalization of the intermediate scattering function to the molecular case is the tensorial quantity

$$S_{lmn;l'm'n'}(\bar{q},t) = \frac{1}{N}\langle \delta\rho^*_{lmn}(\bar{q},t)\,\delta\rho^*_{l'm'n'}(\bar{q})\rangle. \tag{9}$$

These correlators are directly related to experimental quantities [26]; for $l = l' = 0$, they describe the dynamics of translational degrees of freedom that can be measured by neutron scattering when looking at the center of mass low-frequency part of the spectrum; if the molecules possess a permanent dipolar moment, the correlators with $l = l' = 1$ give information related to dielectric measurements and $l = l' = 2$ is finally related to the orientational contribution to light scattering. At this stage, provided the static angular correlators $S_{lmn;l'm'n'}(\bar{q},0)$ and the number density, it is possible to give a closed set of equations for the matrix **S** that completely solve the problem of a liquid of rigid molecules.

The problem is that MMCT seems to be not enough for a high structured molecular system like OTP; we will see that it is not possible to explain some features of the momentum dependence of the structural dynamics without taking into account the internal degrees of freedom (i.e., rotations of the side rings with respect to the central one) that turn out to be strongly coupled to the long-time behavior of the density fluctuations.

III. MODEL AND COMPUTATIONAL DETAILS

In this section we give a brief description of the model and we refer the reader to Ref. [15] for details.

In our model, the OTP molecule is constituted by three rigid hexagonal rings of side $L_a = 0.139$ nm representing the phenyl rings; two adjacent vertices of the central ring are bonded to one vertex of the two lateral rings by bonds of equilibrium length $L_b = 0.15$ nm. In the isolated molecule equilibrium position, the two lateral rings lie in planes that form an angle of about 54° with respect to the central ring's plane. In the model the two lateral rings are free to rotate along the molecular bonds, to stretch along the bonds, and to tilt out of the plane identified by the central ring. The intramolecular potential is then written as a sum of harmonic and anharmonic terms, each one controlling one of these features. Every term is multiplied by a coupling constant whose actual value is determined in order to have a realistic isolated molecule vibrational spectrum. The intermolecular interaction is of the site-site Lennard-Jones type; each of these sites corresponds to a vertex of a hexagon and is occupied by a fictious atom of mass $M_{\mathrm{CH}} = 13$ amu representing a carbon-hydrogen pair. The actual values of the parameters σ_{LJ} and ϵ_{LJ} have been fixed in order to have the first maximum of the static structure factor $S(q)$ in the experimentally determined position [29] and to obtain the correct diffusional properties [20,21]; the cutoff has been fixed to the value $r_c = 1.6\ \mathrm{nm}^{-1}$. It is worth noting here that obviously the parametrization of the potential cannot be perfect; in our case it is possible to reproduce quite well the experimental results on the whole investigated temperature range shifting the MD thermodynamical points at temperatures of 20 K above their true values. The MD simulated system is composed of 108 molecules (324 phenyl rings for a total of 1944 Lennard-Jones interaction sites); at each time step the intramolecular and intermolecular interaction forces are calculated and the equation of motion for the rings are solved for the translational and rotational parts separately.

Wide temperature and momentum ranges have been investigated for values of temperature $380 \leqslant T \leqslant 440$ K and momentum $2 \leqslant q \leqslant 30\ \mathrm{nm}^{-1}$ (the runs details are shown in Table III of Ref. [15]) and the total simulation time is of almost a hundred nanoseconds.

IV. MOLECULES AND PHENYL RINGS

The *collective* density fluctuations dynamics is embedded in the *coherent intermediate scattering function* in general defined as

$$F_t(q,t) = \frac{1}{NS(q)}\left\langle \sum_{i=1}^{N}\sum_{j=1}^{N} \exp -i\bar{q}\cdot[\bar{x}_i(t) - \bar{x}_j(0)] \right\rangle \tag{10}$$

where N is the number of molecules involved and $S(q)$ the static structure factor. In the present case the position variables $x_k(t)$ can be identified with different quantities; here

we are interested in the dynamics of the molecular and phenyl-ring centers of mass so that we will consider the following scattering functions

$$F_t^{(M)}(q,t)=\frac{1}{N_M S^{(M)}(q)} \times\left\langle \sum_{\xi'\xi''} \exp -i\bar{q}\cdot[\bar{M}_{\xi'}(t)-\bar{M}_{\xi''}(0)]\right\rangle, \tag{11}$$

$$F_t^{(R)}(q,t)=\frac{1}{N_R S^{(R)}(q)} \times\left\langle \sum_{ij}\sum_{\xi'\xi''} \exp -i\bar{q}\cdot[\bar{R}_{i\xi'}(t)-\bar{R}_{j\xi''}(0)]\right\rangle. \tag{12}$$

Here $\bar{M}_{\xi'}(t)$ is the position of the center of mass of the molecule ξ' at time t ($\xi'=1,\ldots,N_M$), $\bar{R}_{i\xi'}(t)$ is the position of the center of mass of the phenyl ring i ($i=1,\ldots,3$) pertaining to the molecule ξ'; the functions are renormalized to the corresponding static structure factors. From now on, the superscripts (R) and (M) will refer to rings and molecular quantities, respectively.

As in the case of the incoherent scattering function, at every temperature investigated we have reconstructed the whole curve, even on very-short-time scales, by means of two sets of system configurations campionated with different frequencies (see Table III of Ref. [15]). At every investigated temperature, we considered the momentum values $q_1=14\ \mathrm{nm}^{-1}$ and $q_2=19\ \mathrm{nm}^{-1}$ corresponding to the first and second peak of the experimental static structure factor, averaging on the values of q falling in the interval $q\pm\Delta q$ with $\Delta q=0.2\ \mathrm{nm}^{-1}$. Moreover, the momentum dependence of the principal dynamical parameters has been investigated at $T=280$, 300, and 330 K for values of momenta ranging from 2 to 30 nm^{-1}.

We made a long-time analysis in terms of the usual stretched exponential form of Eq. (4) determining the temperature and momentum dependence of the fitting parameters τ_α, β_α, and f_q and verifying the TTSP.

In Fig. 1 we show $F_t^{(R)}(q,t)$ calculated at q_1 for the temperatures $T=280$, 300, 320, 350, 370, 390, 410, and 430 K (from top to bottom); as in the case of the self-dynamics, every curve decays to zero in the considered time window and the two-step decaying pattern is clearly visible. The long-time part of these $F_t^{(R)}$ have been fitted to Eq. (4) and the parameters τ_α, β_α, and f_q are determined by a least-squares fitting routine. In the inset we plot the same curves as a function of the rescaled time $\bar{t}=t/\tau_\alpha^{(R)}$; all the curves collapse pretty well on a single master curve as predicted by the TTSP. The temperature dependence of the nonergodicity parameter $f_q^{(R)}$ (top panel) and of the stretching parameter $\beta_\alpha^{(R)}$ (bottom panel) are shown in Fig. 2; they are temperature independent—in the limit of our error bars—as predicted by MCT. The mean values $f_q^{(R)}=0.78$ and $\beta_\alpha^{(R)}=0.83$ (dashed line) have to be compared with the values determined in the case of the self-dynamics $f_q\simeq 0.7$ and $\beta_\alpha\simeq 0.8$ [15]. The two values of β_α are equal in the limit of the error bars; at variance, the value for $f_q^{(R)}$ in the collective case is greater than the value found in the one-particle case.

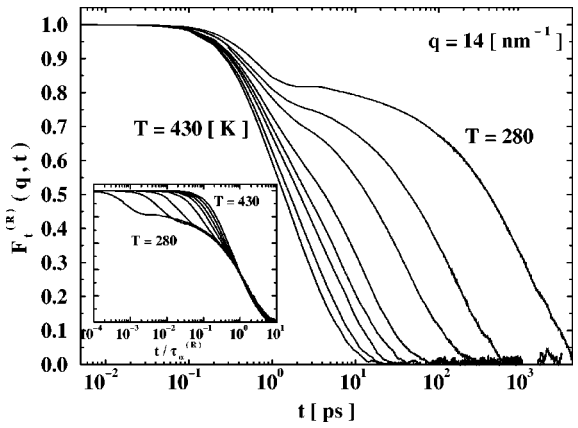

FIG. 1. Intermediate coherent scattering functions $F_t^{(R)}(q,t)$ calculated on phenyl rings at $q=14\ \mathrm{nm}^{-1}$ for the temperatures $T=280$, 300, 320, 350, 370, 390, 410, and 430 K (from top to bottom); in the inset we show the same curves rescaled as a function of $t/\tau_\alpha^{(R)}$.

In Fig. 3 we plot the structural relaxation times at q_1 and q_2 for molecules (triangles and diamonds) and phenyl rings (circles and squares) in order to test if both $\tau_\alpha^{(M)}$ and $\tau_\alpha^{(R)}$ follow the same power law, which is supposed to be momentum independent. Both sets of data have found to be consistent with a power law of the form of Eq. (5) with parameters

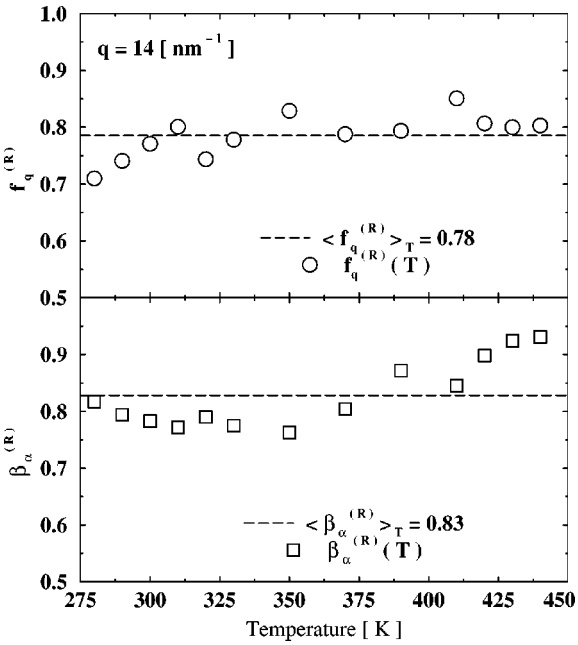

FIG. 2. Temperature dependence of the stretched exponential parameters calculated from $F_t^{(R)}(q,t)$ together with the corresponding mean values (dashed lines). Top: nonergodicity parameter $f_q^{(R)}(T)$. Bottom: stretching parameter $\beta_\alpha^{(R)}(T)$.

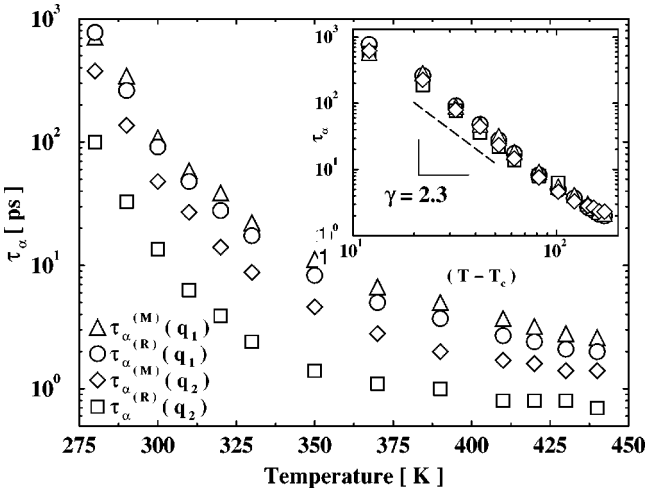

FIG. 3. Temperature dependence of the structural relaxation times at $q_1 = 14\ \mathrm{nm}^{-1}$ and $q_2 = 19\ \mathrm{nm}^{-1}$ calculated both on ring (circles and squares, respectively) and molecule (triangles and diamonds, respectively) centers of mass. In the inset the date are shown in a double-log scale as a function of the rescaled temperature $(T - T_c)$; the points have been shifted in order to maximize the mutual overlap and to stress the power law behavior. The power law of exponent $\gamma = 2.3$ is also shown (dashed line); the value for T_c is 268 K.

$T_c \simeq 268$, $\gamma \simeq 2.3$; these values have to be compared with the results concerning the one-particle dynamics $T_c = 276 \pm 7$ K and $\gamma = 2.0 \pm 0.4$ [15]. The inset show the data plotted as a function of $\overline{T} = T - T_c$, in order to stress the power law dependence, and rescaled by an arbitrary factor in order to maximize the overlap.

We now consider the momentum dependence of the collective dynamics at few selected temperatures $T = 280$, 300, and 330 K, spanning the momentum region in the interval $2-30\ \mathrm{nm}^{-1}$. We test the long-time dynamics in terms of the stretched exponential function and we verify the MCT predictions on the von Schweidler time region, characterized by the power exponent b.

In Fig. 4 we show the stretched exponential fits (solid lines) to $F_t^{(R)}$ at some selected values of q; they work pretty well at least for time values greater than 5 ps. From this figure, it is qualitatively clear that the relaxation time depends non trivially on the momentum values. As we reminded in Sec. II, it is a general property that in the collective case, at fixed temperature, the relaxation times oscillate in phase with the static structure factor, i.e., they are strongly coupled to the static structure of the system.

In Fig. 5 we plot the momentum dependence of the collective relaxation times for molecules (A) and rings (B) at $T = 280$, 300, and 330 K (circles, squares, and triangles, respectively) multiplied by the corresponding diffusion coefficients from Ref. [15]; Eq. (6), which is valid for values of q close to the first maximum of the static structure factor, predicts that these products are temperature independent. In our case the data collapse is not perfect, showing a systematic shift of the data with the temperature. This result is not unexpected due to the fact that Eq. (6) is verified for mono-

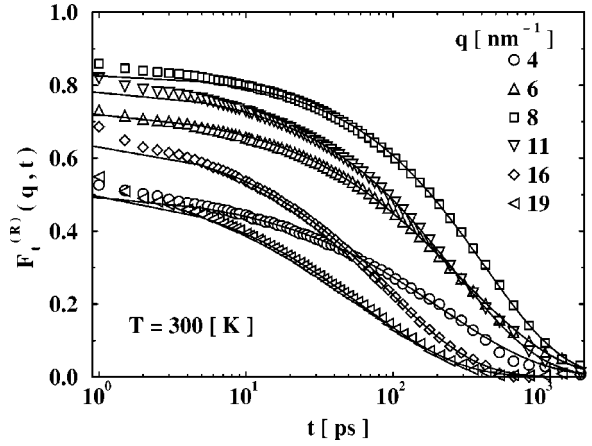

FIG. 4. Intermediate coherent scattering functions $F_t^{(R)}(q,t)$ calculated at fixed temperature $T = 300$ K for different values of momentum q; the corresponding long-time stretched exponential fits are also shown (solid lines).

atomic liquids [28], while for molecular systems some discrepancies have been observed [14].

In the two lower panels of Fig. 5 we plot the corresponding static structure factors divided by q^2 [(c) and (d) for

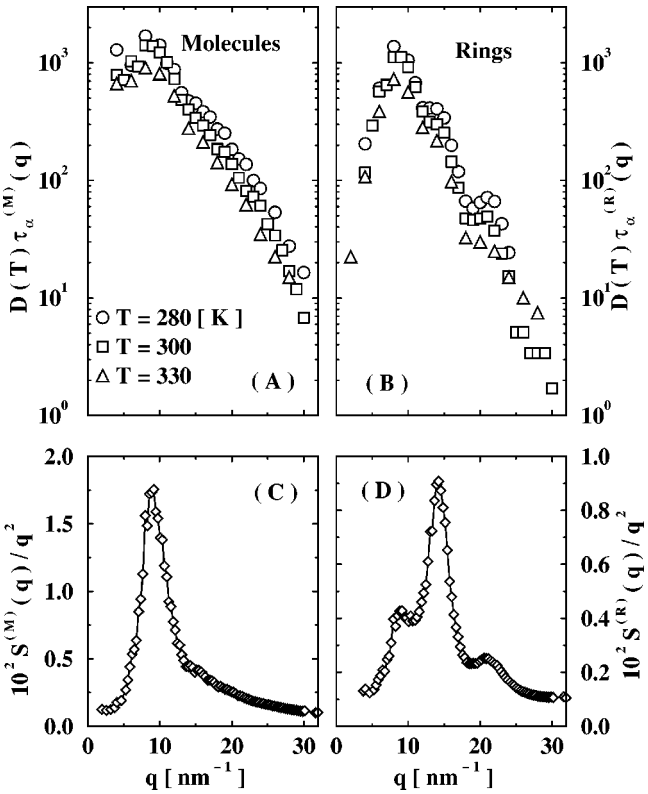

FIG. 5. (a) Structural relaxation times $\tau_\alpha^{(M)}(q)$ for molecules at temperatures $T = 280$, 300, and 330 K (circles, squares, and triangles, respectively) multiplied by the correspondent diffusion coefficients $D(T)$; this product is supposed to be temperature independent. (b) As panel (a) but for $\tau_\alpha^{(R)}$ calculated on phenyl-ring centers of masses. (c) Structure factor calculated on molecular centers of masses divided by q^2. (d) Structure factor calculated on ring centers of masses divided by q^2.

molecules and phenyl rings, respectively]. The correlation among the relaxation times and the respective structure factors of molecules and phenyl rings is evident; it is also evident that, at variance with the temperature dependence, the momentum dependence of the relaxation times is completely different in the two cases.

In the molecular case [Fig. 5(a)] only a maximum at $q \simeq 9\ \mathrm{nm}^{-1}$ corresponding to intermolecular correlations is present (a small shoulder at $q \simeq 14\ \mathrm{nm}^{-1}$, related to correlations between rings pertaining to different molecules, can be also identified). In the case of the phenyl rings [Fig. 5(b)] the momentum dependence is much more structured and three main features are present: (i) a maximum at $q \simeq 9\ \mathrm{nm}^{-1}$ related to correlations between molecular centers of mass; (ii) a shoulder at $q \simeq 14\ \mathrm{nm}^{-1}$ (well developed in a maximum at the lowest temperature, $T = 280$ K) related to correlations between rings belonging to different molecules; (iii) a maximum at $q \simeq 22\ \mathrm{nm}^{-1}$ related to correlations between rings pertaining to the same molecules; this is the most important features related mainly to the orientation of the lateral rings with respect to the central ring.

It is clear from this result that in complex molecular glass formers there are intramolecular rotational and vibrational degrees of freedom that couple to the translational long-time modes as already stressed in Ref. [10]; a theory not taking into account these degrees of freedom cannot explain the whole momentum dependence of the centers of mass dynamics.

In Fig. 6(a) we plot the momentum dependence of the stretching parameter $\beta_\alpha^{(R)}$ at the three selected temperatures $T = 280$, 300, and 330 K (circles, squares, and triangles, respectively) while in panel (b) we show the nonergodicity parameter $f_q^{(R)}$. Also in this case a correlation between the oscillations of these parameters and those of $S^{(R)}(q)/q^2$ [Fig. 6(e)] is somehow clear.

We have seen in Sec. II that the long-time limit of the β region can be described by the von Schweidler power law equations (1), (2), and (3). The exponent b is expected to be momentum independent and to assume the same value of the self-dynamics case, namely, $b = 0.52$ [18]; on the contrary, the amplitude $h(q)$ is expected to be momentum dependent and to oscillate out of phase with the static structure factor. We then calculated a power law fit in the form $F_t^{(R)}(q,t) = f_q^{(R)} - c_2^{(R)}(q) t^{b^{(R)}}$ for all values of momentum considered, in a time window depending on the particular q value but always included in the interval 2–30 ps; moreover, we considered the three parameters free as in the case of the self-dynamics. All the observations done in the previous work concerning the great uncertainties on the estimated values of the fitting parameters hold in the present case. In Fig. 6(c) we plot the power exponent $b^{(R)}(q)$ that is supposed to be momentum independent; some smooth oscillations are nevertheless present but this can be due to the interplay during the fitting procedure with the other oscillating parameters.

In Fig. 6(d) we finally plot the quantity $1/c_2^{(R)}(q)$; in this case some oscillations can be recognized but the noise prevents us from reaching any conclusion. It is worth noting that the values of the nonergodicity parameter $f_q^{(R)}$ calculated by

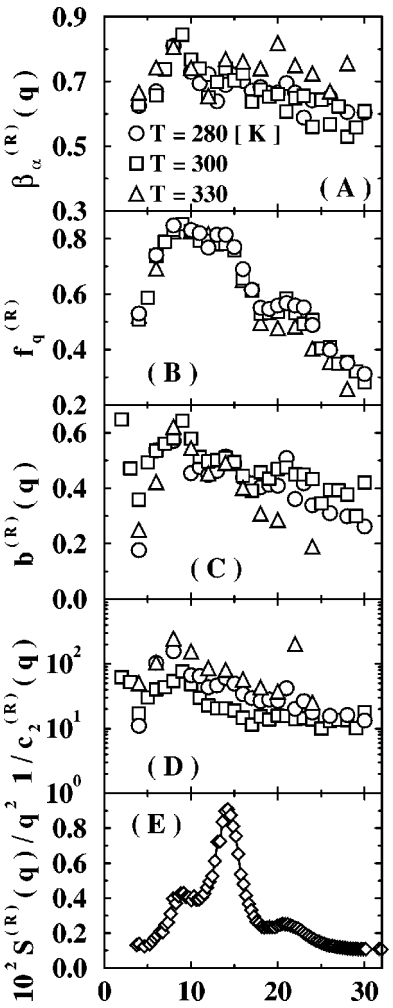

FIG. 6. Momentum dependence of the stretching parameters $\beta_\alpha^{(R)}$ (a) and $f_q^{(R)}$ (b) as calculated by the stretching exponential fit. Also shown are the momentum dependencies of the fitting parameters for the β region $b^{(R)}(q)$ (c) and $1/c_2^{(R)}(q)$ (d). Oscillations in phase with the structure factor (e) are somehow evident.

the von Schweidler law is consistent with the one reported in panel (b). The value of the plateau, indeed, must be the same if determined as the small-time limit of the α region or the long-time limit of the β process.

V. NEUTRON SCATTERING

Neutron scattering is one of the most powerful tools used in the study of supercooled liquids and glasses in the q region covered by the MD simulations. Experimentally the scattering function $F_t(q,t)$ of Eq. (10) can be determined [9] by neutron scattering experiments either directly on neutron spin echo instruments, or by Fourier transforming the dynamical structure factor $S(q,\omega)$,

$$\frac{S(q,\omega)}{S(q)} = \frac{1}{2\pi\hbar}\int dt e^{-i\omega t} F_t(q,t) \tag{13}$$

calculated by means of triple axis backscattering or time-of-

flight spectroscopy. The experimental neutron scattering cross section ($d\sigma/d\Omega dE$) is generally composed of a *coherent* and an *incoherent* part

$$d\sigma/d\Omega dE \simeq \langle b\rangle^2 S_{coh}(q,\omega) + [\langle b^2\rangle - \langle b\rangle^2] S_{incoh}(q,\omega) \tag{14}$$

where b is the scattering length and the symbol $\langle\rangle$ denotes an average over the distribution of nuclear spins and isotopes. The isotopic composition of the sample allows us to study selectively the collective motion via coherent scattering from deuterated samples (the scattering lengths of *D* and *C* atoms are basically coincident) and the one-particle motion via incoherent scattering from protonated samples.

The interaction of neutrons with a bulk sample of OTP can be simulated numerically taking into account the interactions of neutrons with both carbon (C) and deuterium (D) atoms. H atoms are not considered in our dynamics but it is a reasonable approximation to put them in fixed positions on the line extending from the center of the ring through a carbon atom at the fixed C-H distance $d_{\text{C-H}}=0.107$ nm; so that, knowing the coordinates of the rings, it is trivial to reconstruct their own positions. We then define a neutron (N) coherent scattering function $F_t^{(N)}(q,t)$ as

$$F_t^{(N)}(q,t) = \frac{1}{N_A S^{(N)}(q)} \times \left\langle \sum_{\lambda'\lambda''} \sum_{ij} \sum_{\xi'\xi''} b_{\lambda'} b_{\lambda''} \times \exp -i\bar{q}\cdot[\bar{r}_{\lambda' i\xi'}(t) - \bar{r}_{\lambda'' j\xi''}(0)] \right\rangle \tag{15}$$

where $N_A = N_{\text{C}} + N_{\text{H}}$ (3456 in this case) is the total number of atoms, $\bar{r}_{\lambda' i\xi'}(t)$ is the position of the atom λ' pertaining to the ring i in the molecule ξ', and $S^{(N)}(q)$ is the static structure factor of Fig. 11 of Ref. [15]. The number of hydrogen atoms is four for each central ring and five for each lateral ring. The scattering lengths b_λ are, in principle, different for the carbon and deuterium atoms but, as we observed in Ref. [15], they are both positive and of the same magnitude, so that is a good approximation to consider the product $b_{\lambda'} b_{\lambda''}$ an ineffective positive constant. The function $F_t^{(N)}(q,t)$ is the quantity directly comparable with the experimental data.

In the present section we present a comparison between the temperature and momentum dependencies of the MD and experimental spectra of Ref. [11] calculated from perdeuterated $C_{18}D_{14}$ by means of coherent neutron time-of-flight and backscattering spectroscopy.

At this stage few observations must be made on the momentum dependence of the MD and experimental sets of data. All these data are supposed to depend on the structure of the systems so that, in general, some differences are expected (experimental and MD structures are slightly different [15]). Anyway, two observations about the experimental results must be made. First of all, as reported in Ref. [11], some reservation is necessary for the experimental data at the smallest momenta, $q \leqslant 6$ nm^{-1}, where f_q tends toward 1. Indeed, in this region one expects significant background from incoherent scattering, which contributes about 15% of the total cross section, and from multiple scattering. Moreover the technique used to determine the values of the dynamical parameters from the experimental data are quite different with respect to the MD computation. Indeed, due to the limited dynamical window of the available spectrometers, in the experimental case a direct fit of the data to the stretched exponential function with three independent parameters is not possible. Based on the observations that $\tau(q) \propto \eta(T)/T$ [$\eta(T)$ is the viscosity at temperature T] and that the line shape is independent of temperature, at fixed momentum q the spectra at different temperatures are rescaled in time to $\bar{t} = t/t_s$ where the scaling time is given by $t_s = \tau_\eta(T)/\tau_\eta$ ($T = 290K$) and $\tau_\eta = \eta(T)/T$. In this way the data converge toward a temperature-independent long-time asymptote; this is the curve actually fitted to the stretched exponential.

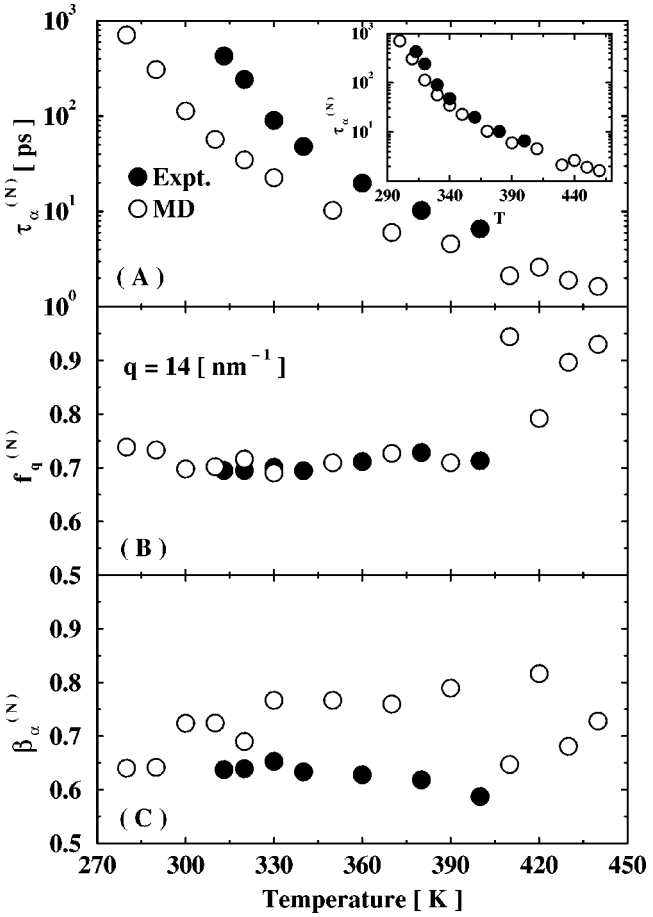

FIG. 7. Comparison among the temperature dependencies of the stretched exponential parameters as calculated by MD simulated neutron spectra (open symbols) and experimental neutron scattering (full symbols) at $q = 14$ nm^{-1}. (a) Relaxation time $\tau_\alpha^{(N)}$; in the inset the MD data have been shifted by 20 K as explained in the text. (b) Nonergodicity parameter $f_q^{(N)}$. (C) stretching parameter $\beta_\alpha^{(N)}$.

In Fig. 7 we show the temperature dependence of the

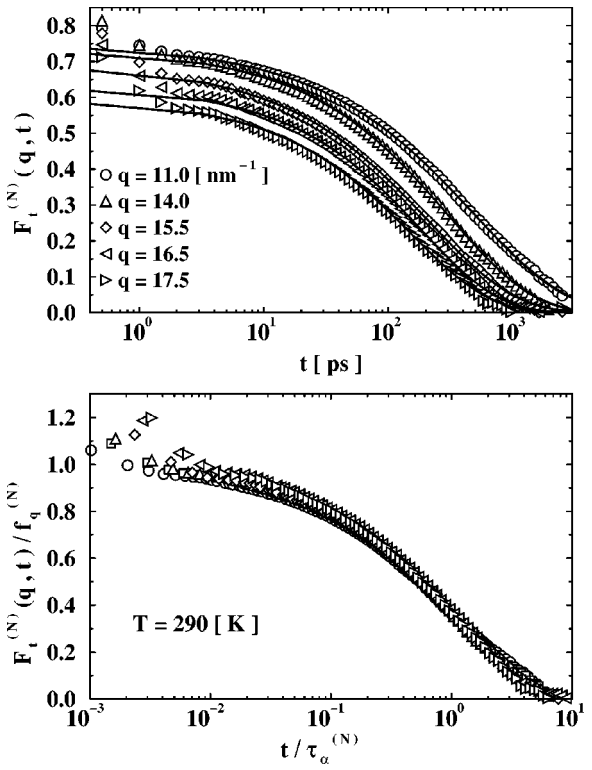

FIG. 8. Top: Simulated neutron coherent scattering function $F_t^{(N)}(q,t)$ at $T=290$ K as a function of momentum. Bottom: $F_t^{(N)}(q,t)/f_q^{(N)}$ plotted as a function of the rescaled time $t/\tau_\alpha^{(N)}$. All the curves collapse on a master curve as expected (in this case $f_q^{(N)}$ depends on q).

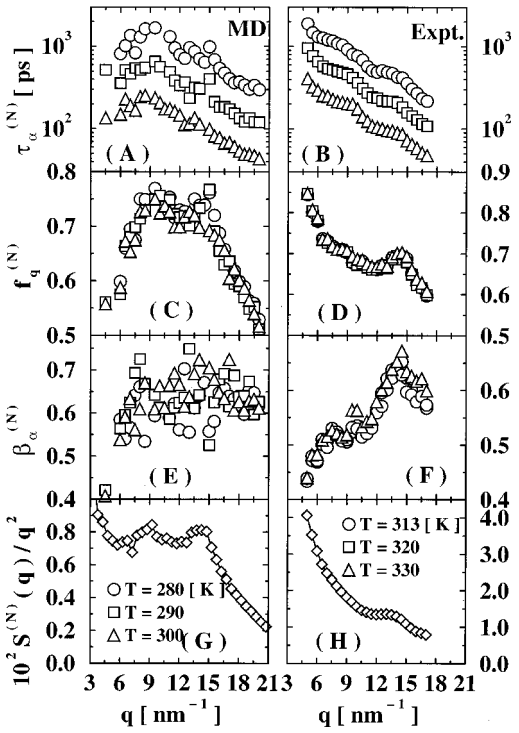

FIG. 9. Comparison among the values of the dynamical parameters calculated by the MD simulations (left panels) and the experimental ones (right panels) together with the appropriate structure factors divided by q^2 [respectively, panels (g) and (h)]. Structural relaxation times $\tau_\alpha^{(N)}$ (a) and (b), nonergodicity parameters $f_q^{(N)}$ (c) and (d), and stretching factors $\beta_\alpha^{(N)}$ (e) and (f).

stretched exponential fitting parameters for the α region of both MD (open circles) and experimental (solid circles) data determined at $q=14\ \mathrm{nm}^{-1}$. In panel (a) we show the structural relaxation times; the inset shows the same data but the MD points have been shifted by 20 K as already explained in Ref. [15]. We stress, indeed, that a nonperfect parametrization of the diffusive behavior of the model system controlled by the value of ϵ_{LJ}, has shifted the MD thermodynamical point about 20 K above the corresponding experimental temperature. From the figure it is clear that the agreement among the two sets of data is very good on a very wide time region. In panel (b) we show our results for the nonergodicity parameter f_q and also in this case the agreement is very good among the two sets of data; in panel (c) we plot the stretching parameters β_α. In this case the MD points are systematically above the experimentally determined data. This effect can be due to the observations made before; moreover, for the determination of the β_α parameter, the very long-time points are crucial and they seem to lack in the experimental data analysis.

With Fig. 8 we start the comparison of the momentum dependence of the two sets of data. In the top panel of Fig. 8 we plot the simulated scattering functions $F_t^{(N)}(q,t)$ (symbols) at $T=290$ K at the indicated q together with the stretched exponential long-time fits (solid lines). In this case $f_q^{(N)}$ is expected to be momentum dependent so that, in order to have a master plot (bottom panel of Fig. 8), we have to show $\overline{F}_t^{(N)}(q,t)=F_t^{(N)}(q,t)/f_q^{(N)}$ as a function of the rescaled time $\overline{t}=t/\tau_\alpha^{(N)}$. The rescaled curves collapse quite well on a master curve as expected. In Fig. 9 we show the comparison for the momentum dependence of the MD data at the three temperatures $T=280$, 290, and 300 K and the experimental data at $T=313$, 320, and 330 K; the two sets of temperatures should be comparable due to the 20-K shift of the MD data. In Fig. 9 we show the MD (left panels) and experimental (right panels) results together with the corresponding static structure factors renormalized to q^2 [panel (g) for MD and (h) for experimental results]. Striking similarities are clear in the case of the structural relaxation times [panels (a) and (b)] even if maxima on MD results correspond to bumps of experimental results. The clearest difference is the decrease of $\tau_\alpha^{(N)}$ at small values of q that appears to be completely absent in the experimental case. This could be due to the incoherent background on the experimental data stressed above; moreover, it is well known that sometimes MD is not able to determine the correct values of τ at small value of q but usually tends to overestimate its correct value, at variance with this case. Anyway, the agreement among the two sets of data at the higher values of q corresponding to the intramolecular correlations is surprising; rigid model could have done that.

In Figs. 9(c) and 9(d) we show the results concerning the nonergodicity parameter $f_q^{(N)}$. The different curves are temperature independent as expected; both sets of data show a

maximum at $q \simeq 14$ nm^{-1}, while the maximum at $q \simeq 9$ nm^{-1} for the MD data correspond to a little shoulder in the experimental case. Also in this case a decreasing part at small q is present in the MD data at variance with the experimental results. But according to Fig. 7 of Ref. [10] the calculation of the nonergodicity parameter fitting the β region gives a plateau at $q \simeq 6$ nm^{-1} at variance with the increasing behavior of the $\alpha-$ region analysis. However, as already stressed in Sec. IV, these data are supposed to coincide. Concluding, also in this case, the experimental data at small q seem to be not reliable.

In Figs. 9(e) and 9(f) we finally show the stretching parameters $\beta_\alpha^{(N)}$. MD data are very noisy, nevertheless it is possible to recognize an oscillatory behavior; moreover, the points at the smallest available value of q seem to catch the decreasing behavior of the experimental data.

VI. SUMMARY AND CONCLUSIONS

In this paper we have concluded the analysis of the long-time center of mass dynamics of the intramolecular model for OTP introduced in Ref. [15]; there we found good agreement among the diffusion properties of the simulated and the real system as well as among the two single-particle dynamics. Moreover in Ref. [15] we found a very good agreement with the main predictions of MCT. In the present paper we definitely confirm such an agreement.

We have studied the collective density fluctuations on a large temperature and momentum range, considering both the fluctuations related to molecular and phenyl-ring centers of mass. With respect to the temperature dependence we found the usual double-step decaying pattern and we confirmed the main predictions of the MCT about the behavior of the stretched exponential parameters; in particular, the relaxation times obey the same power law. The momentum dependence of the stretching parameters appears really interesting; MCT predicts that the behavior in the momentum space of the structural relaxation time, at variance with the trivial square law of the one-particle case, is driven by the structure, namely, it is proportional to $S(q)/q^2$. In both cases, molecules and phenyl rings, this prediction is completely fulfilled. The phenyl-ring behavior is particularly interesting; every feature of the quantity $S(q)/q^2$ is mirrored on the $\tau_\alpha^{(R)}(q)$ curve at the three investigated temperatures $T=280$, 300, and 330 K up to a value of momentum $q \simeq 30$ nm^{-1}. In particular, the maximum at $q \simeq 22$ nm^{-1} is related to fluctuations taking place on molecular length scales; the long-time structural dynamics appears, indeed, coupled to the dynamics of internal molecular degrees of freedom. Similar oscillations are present for the other stretched parameters, and also the correct behavior for the short-time β region is found.

The next step has been a comparison among the experimental and simulated neutron scattering spectra calculated considering both the scattering from carbon and deuterium atoms. The temperature dependences of the relaxation times in both cases are well described by the same power law for almost three decades; a good agreement is also found for the other stretching parameters. The momentum dependence is qualitatively very similar in both cases although some different features not clear are present.

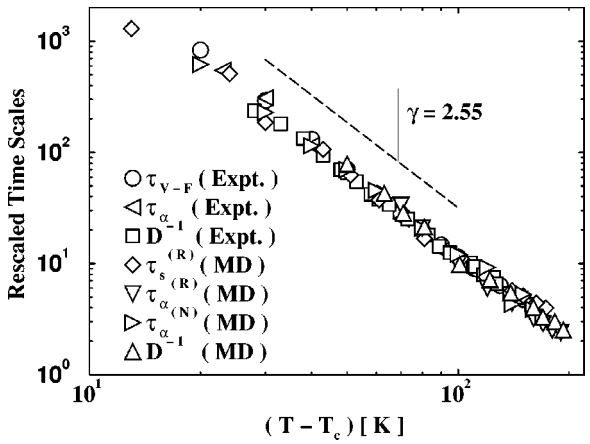

FIG. 10. Master plot of all the time scales related to the center of mass dynamics of the system, calculated by means of molecular dynamics and measured experimentally: experimental viscosity (circles), neutron scattering collective experimental relaxation time (left triangles), and inverse of the experimental diffusion coefficient (squares), MD one particle (diamonds) and structural relaxation time (triangles down) calculated on phenyl rings, MD neutron spectra relaxation time (right triangles), and inverse of the MD diffusion coefficients (triangles up). The data have been rescaled by arbitrary constants in order to maximize the overlap with the viscosity experimental results. All these time scales follow the same MCT power law with exponents $T_c = 290$ K and $\gamma = 2.55$.

At this point some conclusions can be drawn about the capability of our model to describe the long-time dynamics of the real system. All the center of mass time scales calculated by molecular dynamics have been found to be consistent with a power law, although some discrepancies were present for the actual value of the power exponent mainly due to uncertainties on the fitting procedure. Moreover it has been shown that our actual MD thermodynamical point is shifted by about 20 K with respect to the corresponding experimental point. Taking into account all these informations, we plot in Fig. 10 all the time scales related to the centers of mass dynamics considered up to now, both experimental and numerical, as a function of the rescaled temperature $\tilde{T} = T - T_c$ where $T_c = 290$ K [18] for the experimental points and $T_c = 270$ K for the MD results. In particular, $\tau_{V\text{-}F}(T)$ (circles) is the time scale related to the *shear viscosity* η_s of Ref. [30], $\tau_\alpha(T)$ (left triangles) is the neutron scattering structural relaxation time of Ref. [11] at $q = 14$ nm^{-1}, and the inverse of the experimental diffusion coefficient (squares) is from Refs. [20,21]. The MD one-particle relaxation time calculated on phenyl rings $\tau_s^{(R)}(T)$ (diamonds) and self-diffusion coefficient (up triangles) are from Ref. [15]; finally, $\tau_\alpha^{(R)}(T)$ (down triangles) is the structural relaxation time of Fig. 3 calculated at $q = 14$ nm^{-1} on phenyl rings and $\tau_\alpha^{(N)}(T)$ is the simulated neutron scattering relaxation time of Fig. 7. All the data collapse pretty well (although we consider only one decade in temperature) on the same straight line corresponding, on a double-log scale, to a power law of the form of Eq. (5) of exponent $\gamma = 2.55$ [18].

Concluding, our model has been found to be a very successful model for the centers of mass dynamics of the real system, showing a *critical* behavior consistent with the experimental results in a wide time window. The implementation of an intramolecular dynamics is relevant to such an extent; in particular, the internal degrees of freedom appear to be strongly coupled to the long-time structural dynamics as is also clear from the study of the rotational properties of the system [31]. The next step will be the understanding of the role played by the internal degrees of freedom in the fast relaxations observed experimentally [17].

ACKNOWLEDGMENTS

The authors wish to thank F. Sciortino for very useful discussions, J. Wuttke for the raw experimental data of Ref. [11], and L. A. N. Amaral for very useful suggestions.

[1] C. A. Angell, Science **267**, 1924 (1995).
[2] C. A. Angell, K. L. Ngai, G. B. McKenna, P. F. McMillan, and S. W. Martin, J. Appl. Phys. **88**, 3113 (2000).
[3] M. Mézard and G. Parisi, Phys. Rev. Lett. **82**, 747 (1999); J. Phys.: Condens. Matter **12**, 6655 (2000).
[4] W. Götze, in *Liquids, Freezing and the Glass Transition*, edited by J. P. Hansen, D. Levesque, and J. Zinn-Justin (North-Holland, Amsterdam, 1991); W. Götze and L. Sjörgen, Rep. Prog. Phys. **55**, 241 (1992); W. Götze, J. Phys.: Condens. Matter **11**, A1 (1999).
[5] R. Schilling, in *Disorder Effects on Relaxational Processes*, edited by A. Richert and A. Blumen (Springer-Verlag, Berlin, 1994); W. Kob, in *Experimental and Theoretical Approaches to Supercooled Liquids: Advances and Novel Applications*, edited by J. Fourkas *et al.* (ACS Books, Washington, 1997).
[6] W. van Megen and S. M. Underwood, Phys. Rev. Lett. **70**, 2766 (1993); Phys. Rev. E **49**, 4206 (1994).
[7] P. N. Segrè, S. P. Meeker, P. N. Pusey, and W. C. K. Poon, Phys. Rev. Lett. **75**, 958 (1995); P. N. Segrè and P. N. Pusey, *ibid.* **77**, 771 (1996).
[8] Y. Hwang and G. Q. Schen, J. Phys.: Condens. Matter **11**, 1453 (1999).
[9] E. Bartsch, F. Fujara, J. F. Legrand, W. Petry, H. Sillescu, and J. Wuttke, Phys. Rev. E **52**, 738 (1995); **53**, 2011 (1996).
[10] A. Tölle, H. Schober, J. Wuttke, and F. Fujara, Phys. Rev. E **56**, 809 (1997).
[11] A. Tölle, J. Wuttke, H. Schober, O. G. Randl, and F. Fujara, Eur. Phys. J. B **5**, 231 (1998).
[12] P. Gallo, F. Sciortino, P. Tartaglia, and S. H. Chen, Phys. Rev. Lett. **76**, 2730 (1996); F. Sciortino, P. Gallo, P. Tartaglia, and S. H. Chen, Phys. Rev. E **54**, 6331 (1996); F. Sciortino, L. Fabbian, S. H. Chen, and P. Tartaglia, *ibid.* **56**, 5397 (1997); F. W. Starr, F. Sciortino, and H. E. Stanley, *ibid.* **60**, 6757 (1999); C. Y. Liao, F. Sciortino, and S. H. Chen, *ibid.* **60**, 6776 (1999); F. Sciortino, Chem. Phys. **258**, 307 (2000); S.-H Chen, P. Gallo, F. Sciortino, and P. Tartaglia, Phys. Rev. E **56**, 4231 (1997).
[13] L. J. Lewis and G. Wahnström, Phys. Rev. E **50**, 3865 (1994); F. Sciortino and P. Tartaglia, J. Phys.: Condens. Matter **11**, A261 (1999).
[14] A. Rinaldi, F. Sciortino, and P. Tartaglia, Phys. Rev. E **63** 061210 (2001).
[15] S. Mossa, R. Di Leonardo, G. Ruocco, and M. Sampoli, Phys. Rev. E **62**, 612 (2000).
[16] G. Monaco, D. Fioretto, C. Masciovecchio, G. Ruocco, and F. Sette, Phys. Rev. Lett. **82**, 1776 (1999); G. Monaco, S. Caponi, R. Di Leonardo, D. Fioretto, and G. Ruocco, Phys. Rev. E **62**, R7595 (2000).
[17] S. Mossa, G. Monaco, G. Ruocco, M. Sampoli, and F. Sette, e-print cond-mat/0104129; S. Mossa, G. Monaco, and G. Ruocco, e-print cond-mat/0104265.
[18] W. Petry, E. Bartsch, F. Fujara, M. Kiebel, H. Sillescu, and B. Farago, Z. Phys. B: Condens. Matter **83**, 175 (1991).
[19] M. Kiebel, E. Bartsch, O. Debus, F. Fujara, W. Petry, and H. Sillescu, Phys. Rev. B **45**, 10 301 (1992).
[20] D. W. McCall, D. C. Douglass, and D. R. Falcone, J. Chem. Phys. **50**, 3839 (1969).
[21] F. Fujara, B. Geil, H. Sillescu, and G. Fleischer, Z. Phys. B: Condens. Matter **88**, 195 (1992).
[22] J. Wiedersich, T. Blochowicz, S. Benkhof, A. Kudlik, N. V. Surovtsev, C. Tschirwitz, V. N. Novikov, and E. Rössler, J. Phys.: Condens. Matter **11**, A147 (1999).
[23] J. Gapinski, W. Steffen, A. Patkowski, A. P. Sokolov, A. Kisliuk, U. Buchenau, M. Russina, F. Mezei, and H. Schober, J. Chem. Phys. **110**, 2312 (1999).
[24] F. Mezei and M. Russina, J. Phys.: Condens. Matter **11**, A341 (1999).
[25] L. Fabbian, A. Latz, R. Schilling, F. Sciortino, P. Tartaglia, and C. Theis, Phys. Rev. E **60**, 5768 (1999); C. Theis, F. Sciortino, A. Latz, R. Schilling, and P. Tartaglia, *ibid.* **62**, 1856 (2000); L. Fabbian, A. Latz, R. Schilling, F. Sciortino, P. Tartaglia, and C. Theis, *ibid.* **62**, 2388 (2000).
[26] R. Schilling and T. Scheidsteger, Phys. Rev. E **56**, 2932 (1997).
[27] P. G. deGennes, Physica (Utrecht) **25**, 825 (1959).
[28] P. A. Madden, in *Liquids, Freezing and the Glass Transition* (Ref. [4]).
[29] E. Bartsch, H. Bertagnolli, P. Chieux, A. David, and H. Sillescu, Chem. Phys. **169**, 373 (1993).
[30] G. Monaco, Ph.D. thesis, Università di L'Aquila, 1998.
[31] S. Mossa, Ph.D. thesis, Università di L'Aquila, 1999.